TRMM FIRE ALGORITHM, PRODUCTS AND APPLICATIONS

Yimin Ji
School of Computational Sciences
George Mason University, Fairfax, VA 22030, USA

Erich Stocker
NASA/GSFC, Code 902, TRMM/TSDIS, Greenbelt, MD 20770, USA

Abstract. This paper summarizes methodologies of detecting land fires from the Tropical Rainfall Measuring Mission (TRMM) Visible Infrared Scanner (VIRS) measurements. The TRMM Science Data and Information System (TSDIS) fire products include global images of daily hot spots and monthly fire counts at $0.5^o \times 0.5^o$ resolution, as well as text files that details necessary information of all fire pixels. These products have been archived since January 1998. Diurnal and seasonal cycles of TRMM land fire products in the eastern United States, Africa, as well as the South America and Asia, are discussed and compared to other satellite products. Statistical methods were applied to the TSDIS fire products as well as to the Total Ozone Mapping Spectrometer (TOMS) aerosol index products for a period of seven years from January 1998 to December 2004. The variability of global atmospheric aerosol is consistent with the fire variations during this period. The TRMM fire products were also compared to the coincident TRMM rainfall and other rainfall products to investigate the interaction between rainfall and fire. The results indicate that the annual, interannual and intraseasonal variability of fire are dominated by global rainfall variations. However, the feedback of fire to the rainfall occurrence at regional scale for certain regions is also evident.

1. TSDIS FIRE ALGORITHMS

Using measurements of VIRS 3.75 μm and 11 μm bands, the TSDIS fire product algorithm was built on heritage algorithms of NOAA/AVHRR**.** The TRMM/VIRS and NOAA/AVHRR have five channels with similar center wavelengths and bandwidths across visible and infrared spectrums (0.63μm, 1.61 μm, 3.75 μm, 10.8 μm, and 12 μm). VIRS scans a 45-degree swath with a 2.11 km Instantaneous Field of View (IFOV) at nadir and 3.02 km IFOV at the edge of scan from the non-sun-synchronous 350 km TRMM orbit. The VIRS geometric registration has an uncertainty about 0.5 ~ 0.8 of the pixel size. VIRS provides twice daily observation over most of the tropical and subtropical areas (180^oW-180^oE and 40^oS-40^oN).

The fundamental physics of the fire algorithm using VIRS 3.75 μm and 11 μm bands is the Wien displacement law:

$$\lambda max = C/T$$

Where λmax is the wavelength at which the radiation is at a maximum if the radiative temperature is at T. C = 2898 μm·K is a constant. Thus, the vegetated surface over tropics and sub-tropics, with a radiative temperature about 300 K, has a peak around the 11 μm band. Fire pixels, with radiative temperatures about 800 K, have a radiative peak around the 3.75 μm band. Therefore, if fires occur in a portion of a pixel, the radiant energy of 3.75 μm band increases much more rapidly than that of 11 μm band, resulting in a larger than normal difference of brightness temperatures between the two bands. If a large part of a pixel is filled with fires, the 3.75 μm band could be saturated because the saturation temperature of VIRS 3.75 μm band is only around 322 K. We have not observed Saturation of the VIRS 11 μm although the saturation temperature of this band is similar to that of 3.75 μm band. The 11 μm band is not as sensitive as the 3.75 μm band to the thermal anomalies happening within a pixel.

The TSDIS nighttime algorithm is basically a traditional threshold method using only the VIRS thermal band brightness temperatures (Tbs). The TSDIS fire algorithm uses the following criteria to detect nighttime fire pixels:

1. Channel 3 (3.75 μm) is saturated or
2. Tb3 > 315 K and Tb3-Tb4 > 15 K

In general, only a small portion of a pixel may be occupied by the fire when a fire occurs. Because the environmental Tb3 (Tb3env) is about 300 K and the fire Tb3 is about 800 K, the criteria presented above may reject a pixel that has less than 2% of its area occupied by fire.

The daytime algorithm first uses the thermal band Tbs to chose candidate of fire pixels. After that, additional tests are performed to make final choices. These tests use VIRS visible/near-infrared data as well as ancillary data sources. Based on these analyses, the TSDIS daytime fire algorithm uses the following criteria to identify daytime fire pixels:

1. Channel 3 (3.75 μm) is saturated and Tb4 > 285 K or Tb3 > 320 K and Tb3-Tb4 > 20 K and Tb4 > 285 K
2. Pixel is not a bare ground, or open shrub pixel
3. Tb3 - Tb3env > 8 K.

The Tb4 requirement is used to exclude cloud and heavy aerosol pixels. Under these conditions, the algorithm is unable to detect fire pixels.

2. TSDIS FIRE PRODUCTS

TSDIS fire algorithm routinely creates global daily and monthly fire products. The global fire product has a lag time of approximately 14 hours. The daily products include two files. The first file, the basic file of all products, is a text file that details necessary information for all fire pixels. The information includes date, orbit number, pixel number, solar zenith angle, latitude, longitude, UTC time, reflectance of visible/near infrared channels, brightness temperatures of infrared channels, as well as background brightness temperature of infrared channels. This text file is then used to create a global hot spot image that is displayed on the TSDIS home page.

Fig. 1 shows a typical daily hot spot image of April 12 2005. The upper panel displays the distribution of global fire pixels. The three lower panels show enlarged area maps over Northern America, Southern America, and the Indonesian area. On this particular day, a large number of fire pixels were detected over the Southeast Asia and sub-Sahara.

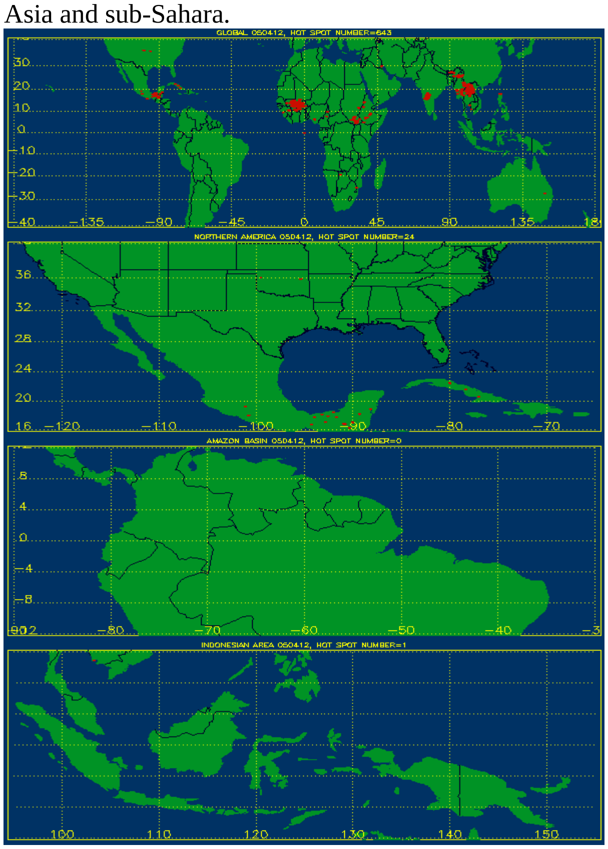

Fig. 1. TSDIS daily hot spot image of April 12, 2005

The monthly image is a $0.5^o \times 0.5^o$ resolution composite of fire counts for the month. The monthly text files provide information for all fire pixels observed within the month. The monthly text files have been reprocessed recently from the beginning of TRMM missing such that overpass time for each fire pixel may be retrieved. Users may download or ftp the description of algorithm, as well as the daily and monthly products (image and data) from TSDIS home page or anonymous ftp site. However, as described in the above section, daytime hot spots contained in these files may contain a large number of false fire pixels. A typical way for user to further exclude false alarms is day/night screening. Such screening may reject most false fires in non-fire season. The detailed description of TRMM fire algorithm and products can be found in Ji and Stocker (2002a).

3. FIRE AND AEROSOL CPMPARISON

Fires may occur randomly but are constrained by the regional climate and vegetation state. The TRMM yearly mean fire count of 1998-2003 years (Fig. 2a) showed intensive fires in South America, Africa, Australia, Southeast Asia, and Indonesia. Moderate fires occurred in China, Northern and Central America. In February, March, April, and May (FMAM) season, most fires occurred in the northern hemisphere (Fig. 2b), especially in Southeast Asia, sub-Saharan Africa and Central America. In June, July, August, and September (JJAS), fires were observed in the southern hemisphere and northern America (Fig. 2c).

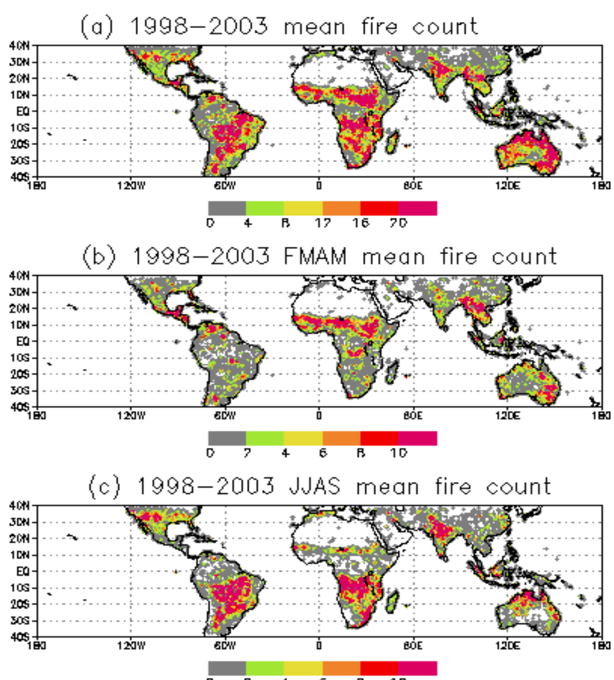

Fig. 2. Global distribution of fire count (resolution: $0.5^o \times 0.5^o$) (a) annual mean from 1998 to 2003. (b) FMAM mean from 1998 to 2003. (c) JJAS mean from 1998 to 2003.

The dominant pattern of aerosol index is the Sahara dust (Fig. 3a). However, the contribution of intensive fires is evident. Since fires occur only in certain season while the Sahara dust is almost a static feature, the magnitude of mean aerosol index in burning areas is significantly smaller than that of the Sahara dust. In FMAM season, the magnitude of aerosol index over fire centers of Southeast Asia and Indonesia is comparable to that over Sahara desert area (Fig. 3b). Fires in these areas have been very serious in the recent decade (Malingreau 1990; Giri and Shrestha 2000). Almost no aerosols were observed over the southern hemisphere in this season. In JJAS season (Fig. 3c), the strength of aerosol index in southern Africa and southern America is quite strong but still considerably weaker than that of Sahara dust. There were moderate aerosols in northern America in this season. The aerosol index maps are generally in agreement with the fire maps except the desert area. The detail of inter-comparison can be found in Ji and Stocker (2002b).

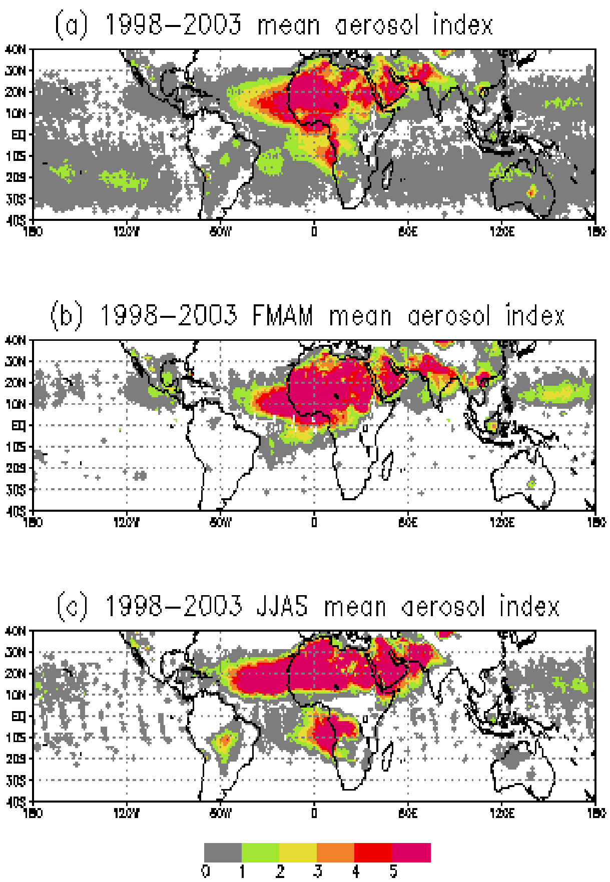

Fig. 3. Global distribution of aerosol index (resolution $1.25^o \times 1.0^o$). (a) annual mean from 1998 to 2003. (b) FMAM mean from 1998 to 2003. (c) JJAS mean from 1998 to 2003

4. DIURNAL AND SEASONAL CYCLES

In order to study the diurnal cycle and seasonal variability, the day/night hot spots must be carefully studied for reliable fire seasons. Fig.4 indicates different pictures of seasonal cycles by using daytime and nighttime satellite fire data. In the eastern USA, the nighttime product shows peaks around April for each year, while the daytime product showed much stronger seasonal cycle. In the western USA, the nighttime fire counts do not show evident seasonal cycle, but the daytime counts indicate a stong annual cycle with peaks in summer time.

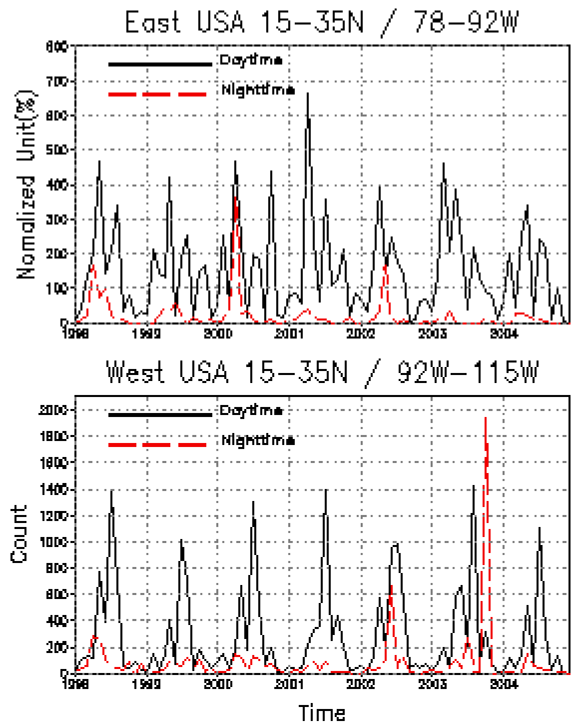

Fig. 4 Daytime and nighttime TRMM fire seasonal variations in East USA (upper) and West USA (lower)

Diurnal variations during spring and summer seasons in the East and West United States are demonstrated in Fig. 5. In East USA, the summer time fire shows strong diurnal cycle with a peak in noon. The spring fire has a peak between noon and 6 pm and last into midnight. The situation is similar for west USA area. In summary, false fire in daytime may impact both daily and seasonal cycles significantly. We have looked into a number of fire regions for the past seven years and found that in fire seasons, the fires are often observed during nighttime (Fig. 6). During an off-fire season, the satellite observation may show hot spots in daytime but not in nighttime.

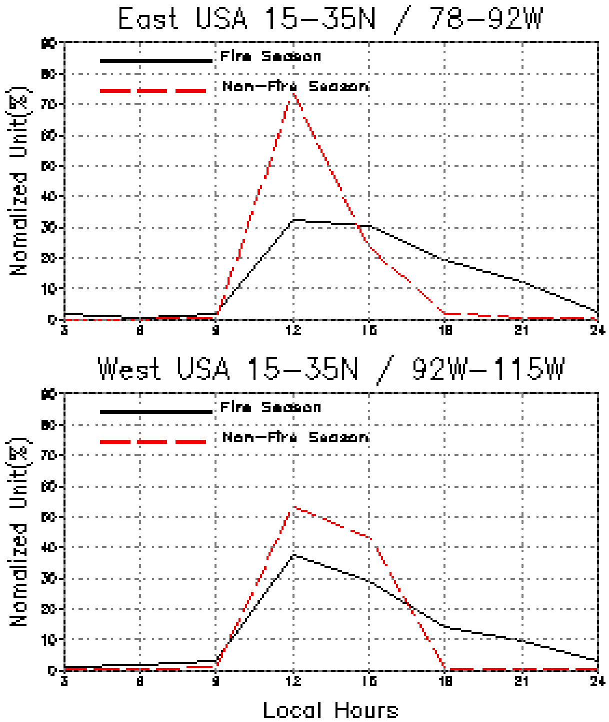

Fig. 5 TRMM fire diurnal cycle in fire and non-fire seasons in East USA (upper) and West USA (lower)

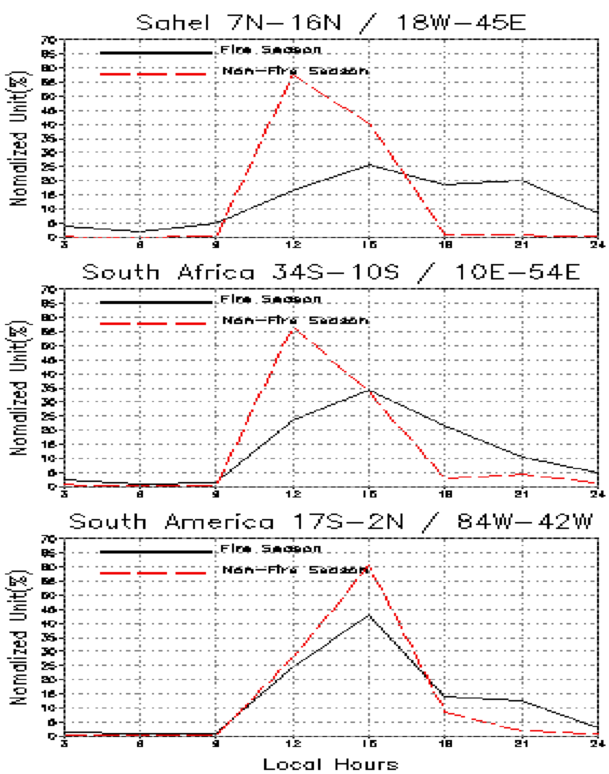

Fig. 2 Comparison of TRMM fire diurnal cycle in fire and non-fire seasons in Sahel area (upper), South Africa (middle), and Indo China (lower)

5. FIRE AND RAINFALL

Time series of TRMM observed fire count (count/day) and transformed fire count (count/day) in Southeast Asia is displayed in Fig. 7. In the observed time series, the effect of satellite aliasing can be seen from a number of dips during certain fire episodes. Such dips are largely eliminated in the transformed time series. The fire time series in Southeast Asia are also compared with the rainfall over land. The result indicates that the fire seasonal and intraseasonal variability are closely related to the rainfall variations.

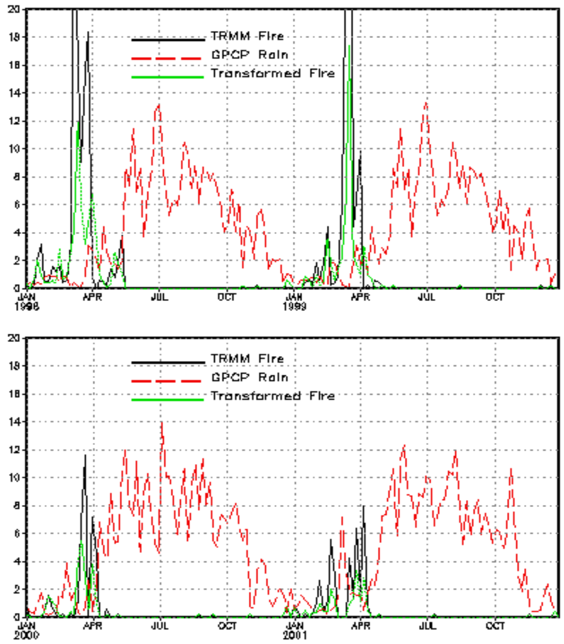

Fig. 7. Time series of TRMM fire count(count/day, solid line), TRMM transformed fire count (count/day, dotted line), and GPCP rainfall (mm/day) in Southeast Asia (90°E- 110°E, 5°N – 25°N)

Although the fire season and variability are dominated by global rainfall variations, the positive feedback from cloud microphysics on the land fire has been suspected for many years. The hypothesis is that the large concentration of small CCN in the smoke from fire nucleates many small cloud droplets that coalesce inefficiently into the raindrops.

References

Ji Y, Stocker E (2002a) An overview of the TRMM/TSDIS fire algorithm and products. *Int. J. of Remote Sensing* **23**: 3285-3303

Ji Y, Stocker E (2002b) Seasonal, Intra-seasonal, and Interannual Variability of Land Fires and their effect on the Atmospheric Aerosols. *J. of Geophys. Res.* **107**: 4697, doi: 10 1029/2002JDoo2331.